Layer-by-layer Assembly into Bulk-like g-C$_3$N$_4$ via Artificially Manipulating Electrostatic Force

Yan Wang[a], Guangshe Li[a,*], Yuelan Zhang[a], Liping Li[a,*], Mingyu Shang[b]

*Corresponding author. E–mail: lipingli@jlu.edu.cn; guangshe@jlu.edu.cn

2 Experimental

2.1 Materials

Chemicals of Urea and thiourea were purchased from Sinopharm Chemical Reagent Co., Ltd. hydrochloric acid was purchased from Beijing Innochem Co.. N,N-dimethylformamide (DMF) was purchased from Tianjin Tiantai Co. Ethanol (99.7%) was purchased from Beijing chemical works. All chemicals were analytical grade and used without any further purification. Deionized water was used throughout this research.

2.2 Synthesis of protonated g-C$_3$N$_4$ nanosheets (PCN)

Urea was calcined at 550 °C for 4 h in nitrogen in a tube furnace to prepare bulk g-C$_3$N$_4$ (BCN). Subsequently, BCN was heated to 500 °C and kept at this temperature for 2 h to obtain g-C$_3$N$_4$ nanosheets. Subsequently, the prepared g-C$_3$N$_4$ nanosheets were dispersed in HCl aqueous solution with ultrasonic treatment for 2 h, and stirred for another 2 h for protonation of sample surface. The protonated g-C$_3$N$_4$ nanosheets (PCN) were filtrated and washed by deionized water to remove residual HCl until the pH =7. Finally, the obtained PCN was dried in oven at 60 °C for 12 h.

2.3 Synthesis of O doped g-C$_3$N$_4$ nanosheets (OCN)

Thiourea was heated to 550 °C for 4 h in air in a tube furnace, the obtained sample named as BOCN. OCN was synthesized by the above mentioned method except that the precursor and the reagent of ultrasonic treatment were replaced with BOCN and DMF, respectively.

2.4 Synthesis of bulk-like g-C$_3$N$_4$

Bulk-like g-C$_3$N$_4$ photocatalyst was prepared by an electrostatic self-assembly method. Firstly, PCN (0.1g) and OCN (0.1g) at the same mass were dispersed in aqueous hydrochloric acid at pH=3 by ultrasonic, respectively. PCN suspension was dripped to OCN suspension drop by drop. The obtained solution was filtrated and washed by deionized water until pH =7. The as-obtained product was dried in oven at 60 ^{o}C for 12 h. The obtained bulk-like g-C$_3$N$_4$ sample was named as PCN/OCN. The other samples containing different mass ratios of PCN to OCN were also prepared by varying the mass of PCN (0.07g and 0.15g) under the same conditions, which were then labeled as PCN/OCN-0.7 and PCN/OCN-1.5, respectively.

2.5 Characterization

X-ray diffraction (XRD) data were recorded by Rigaku MiniFlex 600 at a scan rate 1°/min from two theta of 5° to 60°. TEM and HRTEM were performed by Tecnai F20 electro-microscope from FEI Company operated at 300kV. The microstructure, surface composition and electronic states of the samples were obtained by Fourier transform spectrophotometer (FT-IR, IS 50, Thermo Nicolet), and X-ray photoelectron spectroscopy (XPS) (Thermo ESCALAB 250 spectrometer. Using C1s peak at 284.8 eV as standard). The microstructure was further characterized by the ^{13}C solid-state NMR analysis performed on Bruker-BioSpin AVANCE III HD spectrometer, and the spinning rate was set to 8 kHz. The UV-vis diffuse reflectance spectra (UV-vis DRS) (U-4100) were measured at 200-800 nm. The photoluminescence (PL) spectra were recorded by fluorescence spectrometer (LS5). Zeta potential were recorded by Laser Nanometer Particle Size Analyzer (Zetasizer-Nano-ZS, British Malvern Instrument Co., Ltd.) under pH=3 at 25 ^{o}C. Adsorption-desorption isotherms of N$_2$ for samples were measured using TriStar 3000 (Micromeritics) nitrogen adsorption apparatus at 77 K. Morphologies of the samples and the elemental distributions were obtained by field scanning electron microscopy (SEM) (JSM-6700F) and SEM mapping.

2.6 Photocatalytic H$_2$ evolution reaction

The photocatalytic water splitting tests were performed using 200 mL pyrex glass reaction cell at a reaction temperature of 5 ^{o}C controlled by circulating condensing unit, the light source choose 300 W Xe lamp equipped with a total reflection (λ=320-780

nm), cut-off filter ($\lambda > 420$nm) and simulated sunlight filter (AM1.5G). Photocatalyst (0.05 g) was dispersed to the mixed aqueous solution containing 45 mL deionized water and 5 mL TEOA solution as well as 0.15 mL H_2PtCl_6 solution (1wt% Pt). The amount of H_2 was determined by the gas chromatograph (GC-7900).

After 8 h measurement of photocatalytic H_2 generation, the samples were collected by centrifugation, washed with deionized water several times, and then dried in an oven at 60 ^{o}C for 12 h for the next cycle test.

The apparent quantum yield (AQY) was calculated to find out the energy conversion efficiency of the as-synthesized samples. The photocatalytic mixtures were irradiated by an incident Xe light source with filters (λ = 350, 400, 420, 450 and 500 nm) at 5 ^{o}C. AQY calculation was carried out with following equation:

$$AQY = \frac{2*n(H_2)}{Number\ of\ incident\ photons} = \frac{2*n(H_2)}{IA\lambda/hc} * 100\%$$

where n(H_2) is the number of produced H_2 molecules per second, I is the power of light source (W/cm^2) over the irradiated area A (cm^2), λ is the wavelength of the light, h is Planck's constant and c is the speed of light. The turnover numbers (TON) for the photocatalytic water splitting was measured when the photocatalytic reaction reached the platform,

$$TON = \frac{the\ molar\ amount\ of\ gas\ production}{the\ molar\ amount\ of\ catalyst}$$

2.7 Photoelectrochemical measurements

Mott-Schottky (MS) plots were recorded using an electrochemical work station (CHI760D instruments) in a standard three-electrode system equipped with as-prepared samples, Ag/AgCl (saturated KCl) and a Pt sheet as the working electrode, reference electrode and counter electrode, respectively. The applied alternative current (AC) frequency is 1000, 2000 and 2500 Hz. The working electrodes were obtained as follows: 3.5 mg sample was dispersed in the mixed solution of 0.05 mL nafion aqueous solution (5 wt%) and 0.45 ml ethanol. After 30 min of ultrasound, the suspension was uniformly coated on the 2 cm × 1.5 cm FTO glass electrode. Then, the obtained electrode was dried naturally. Electrochemical impedance spectroscopy (EIS) was

performed with the same three-electrode system and conducted in testing frequency range from 0.01 to 1×10^6 Hz with amplitude 5 mV. Photocurrent was performed at open circuit potential under Xe lamp illumination (320-780 nm). All these polarization curves are compensated by ohm.
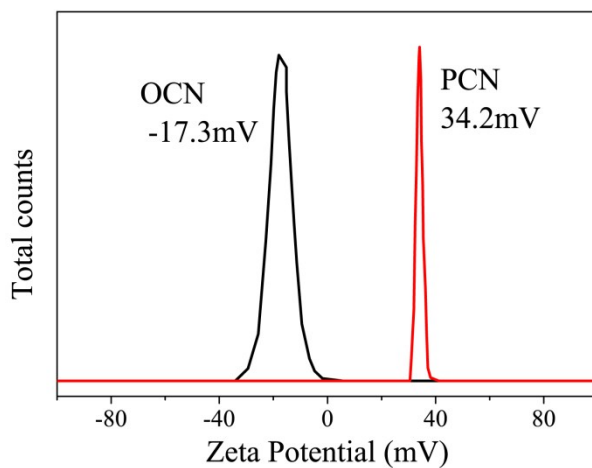

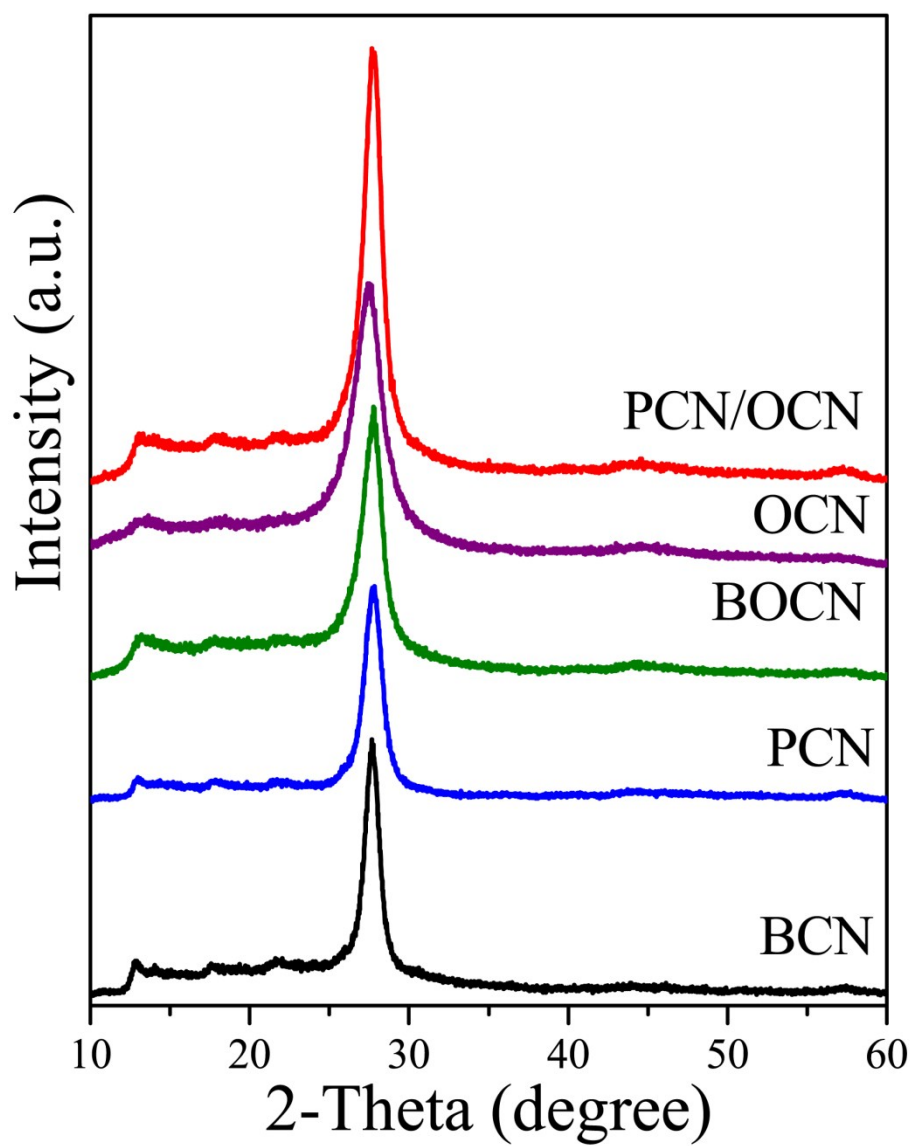Figure S1. Zeta potentials of PCN and OCN at pH=3

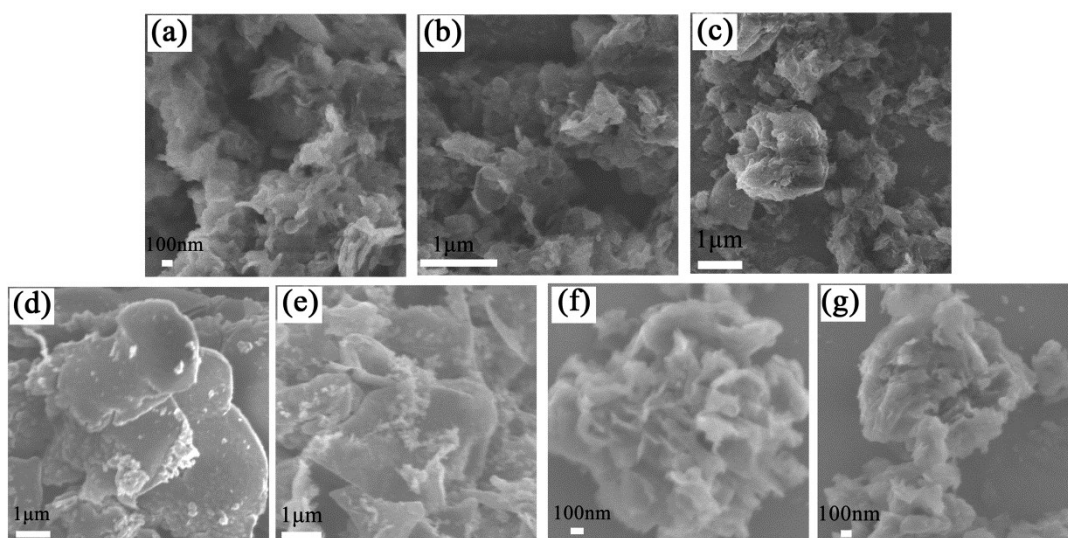Figure S2. XRD patterns of the given samples.

Figure S3. SEM images of the samples: (a) PCN/OCN, (b) PCN/OCN-0.7, (c)PCN/OCN-1.5, (d) BCN, (e) BOCN, (f) PCN, and (g) OCN.
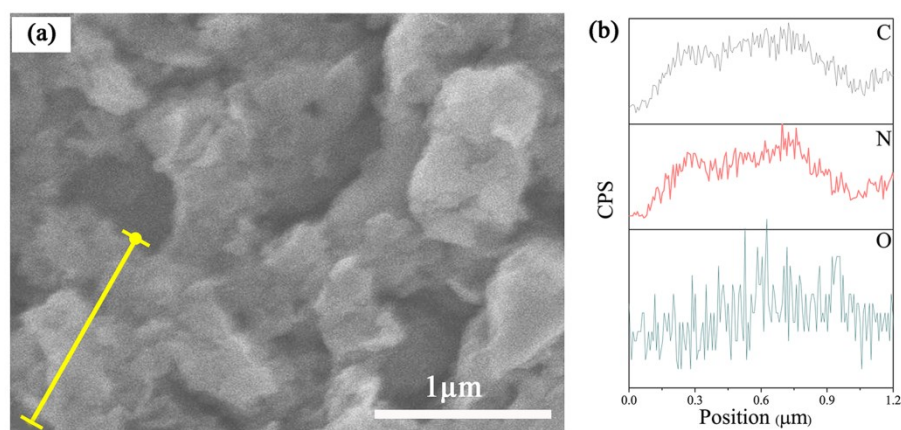
Figure S4. (a) SEM image and (b) elemental distributions of C, N and O along with the yellow line for bulk-like PCN/OCN.

Morphologies and elemental distribution of PCN/OCN were examined by SEM and elemental mapping analysis. As shown in Figure S3, PCN/OCN, PCN/OCN-0.7 and PCN/OCN-1.5 showed a structure constructed by thin nanosheets. Comparatively, BCN and BOCN consisted of large nanosheets with slightly smooth surfaces. These results can be also confirmed by TEM observations for PCN/OCN and BCN (Figure S5). After protonation and oxygen doping, the surfaces of PCN and OCN were rugged. C, N and O distribution profile of EDS line scanning for PCN/OCN in Figure S4 indicated that PCN and OCN were successfully combined.
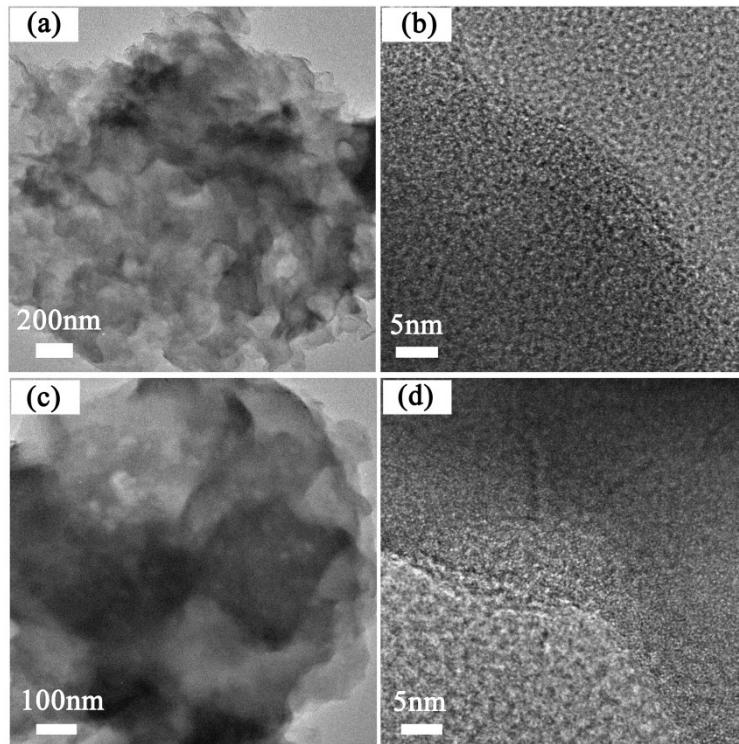
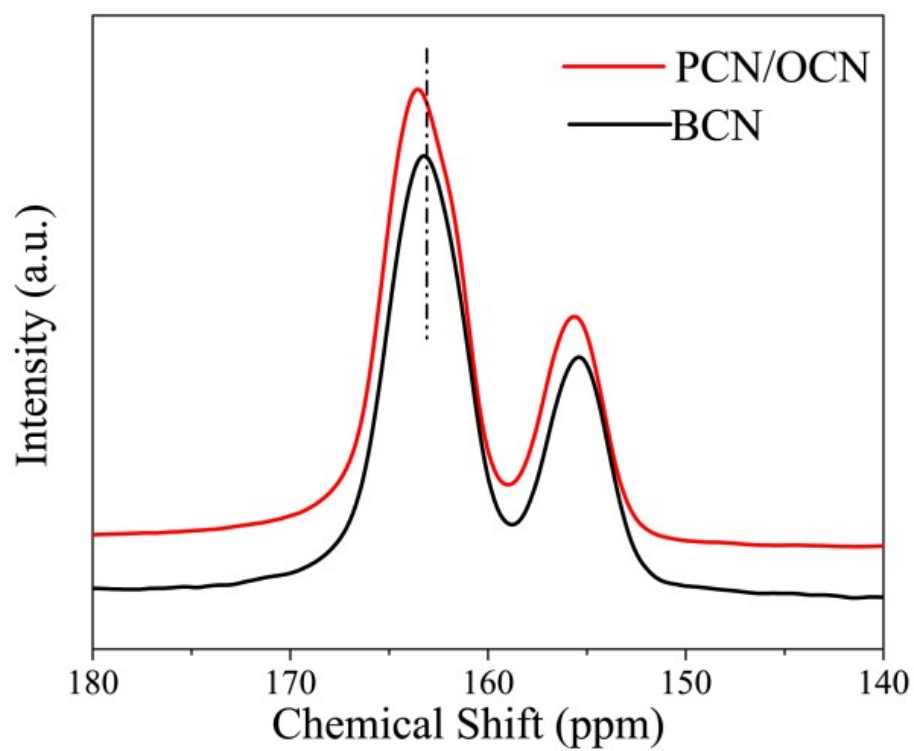Figure S5. TEM and HRTEM images of the samples: (a, b) PCN/OCN and (c, d) BCN.

Figure S6. ^{13}C NMR for samples PCN/OCN and BCN. Two signals ranging from 150 ppm to 160 ppm and from 160 ppm to 170 ppm are ascribed to heptazine carbon, CN_3, and terminated NH_2 and NH groups ($CN_2(NH_x)$), respectively.
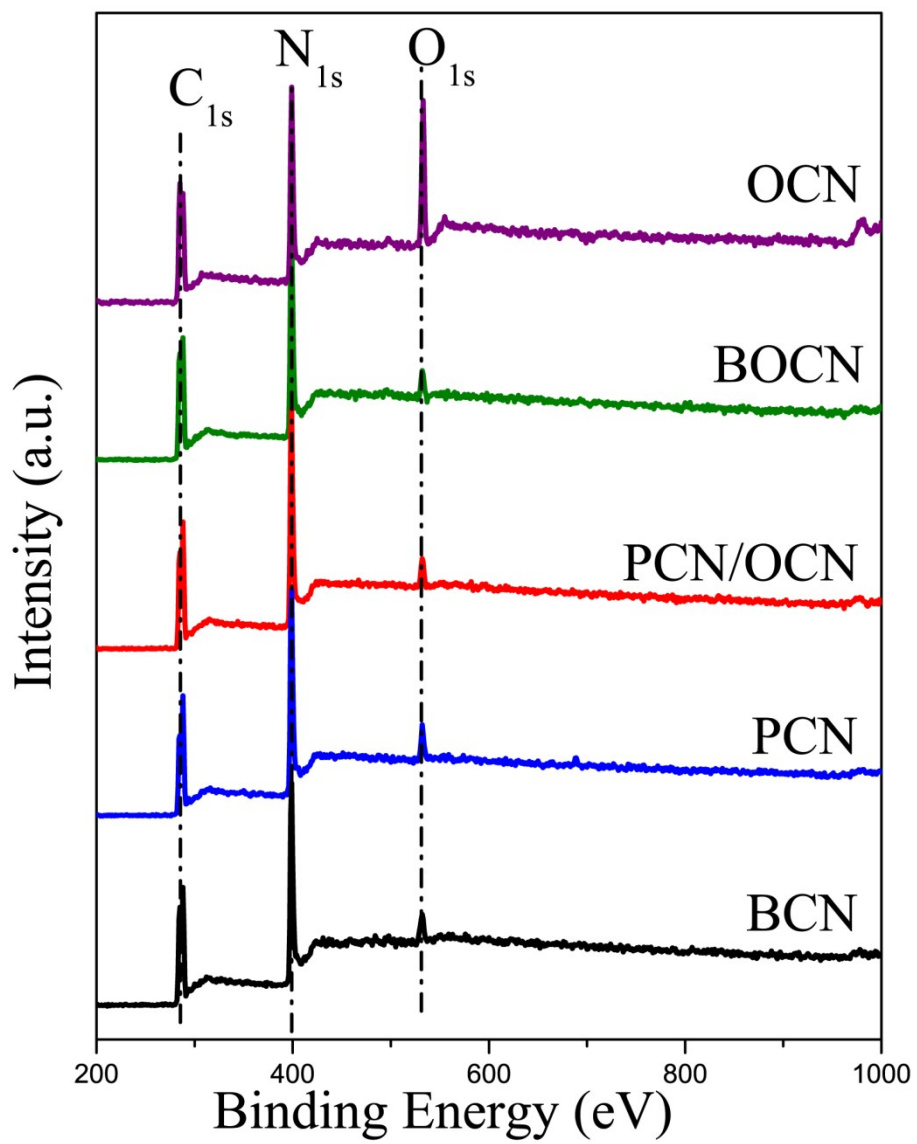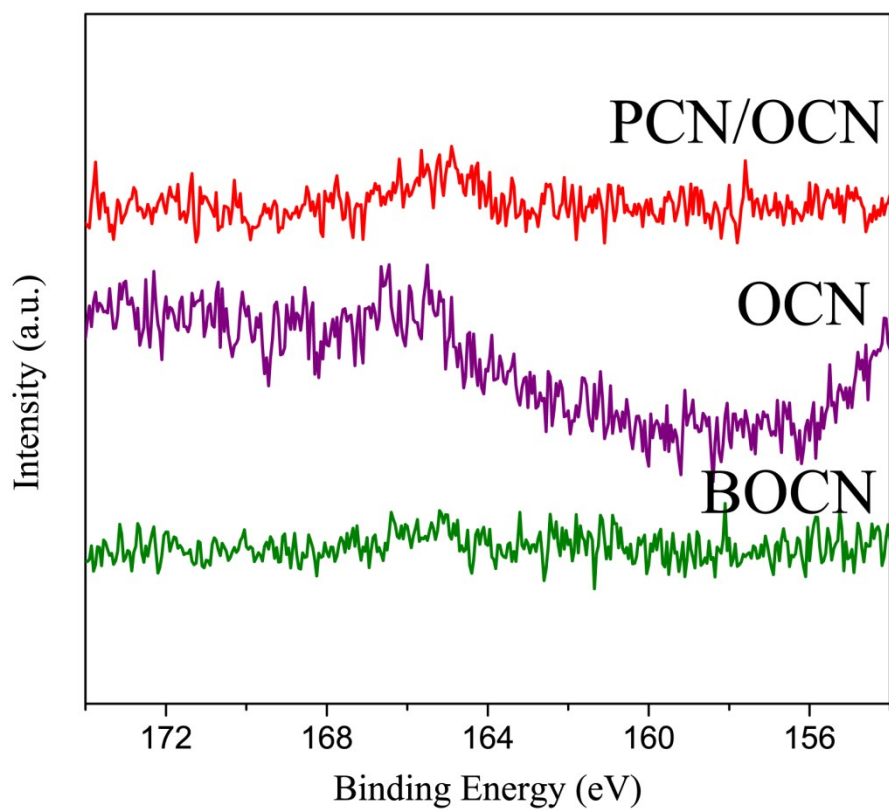
Figure S7. XPS survey spectra of the given samples.

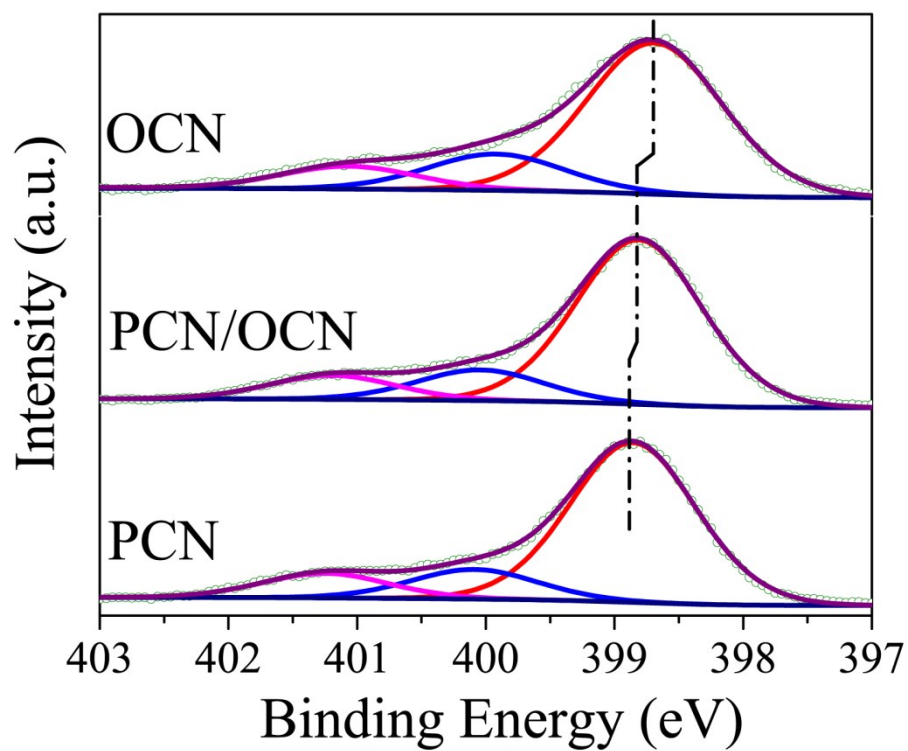Figure S8. High resolution spectra of S2p XPS for OCN, BOCN and PCN/OCN samples.
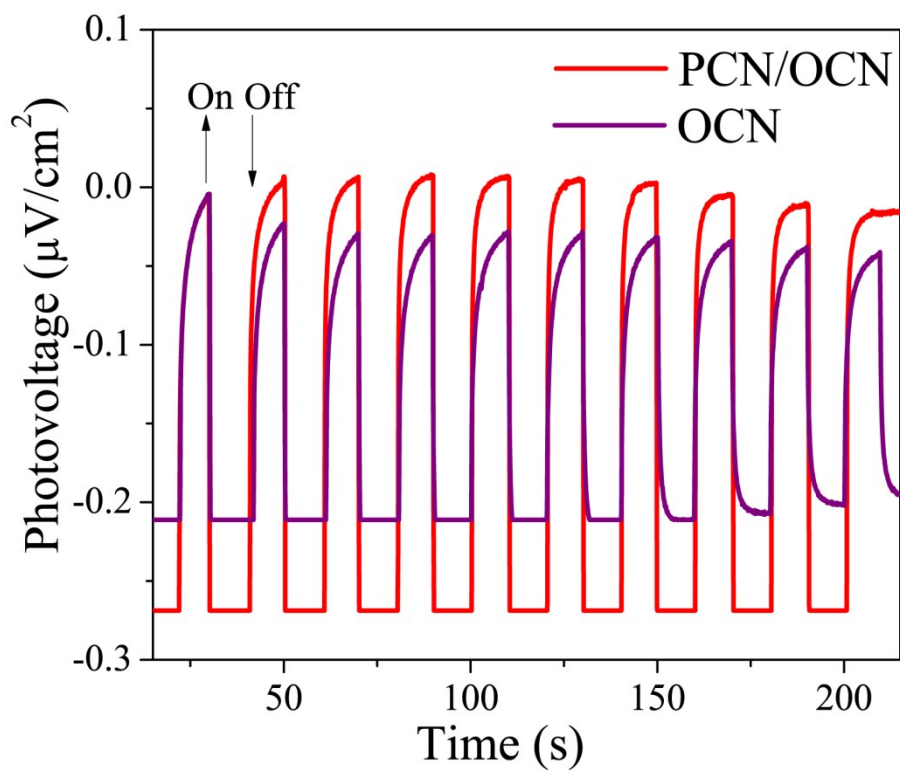

Figure S9. N 1s spectra of OCN, PCN and PCN/OCN samples.
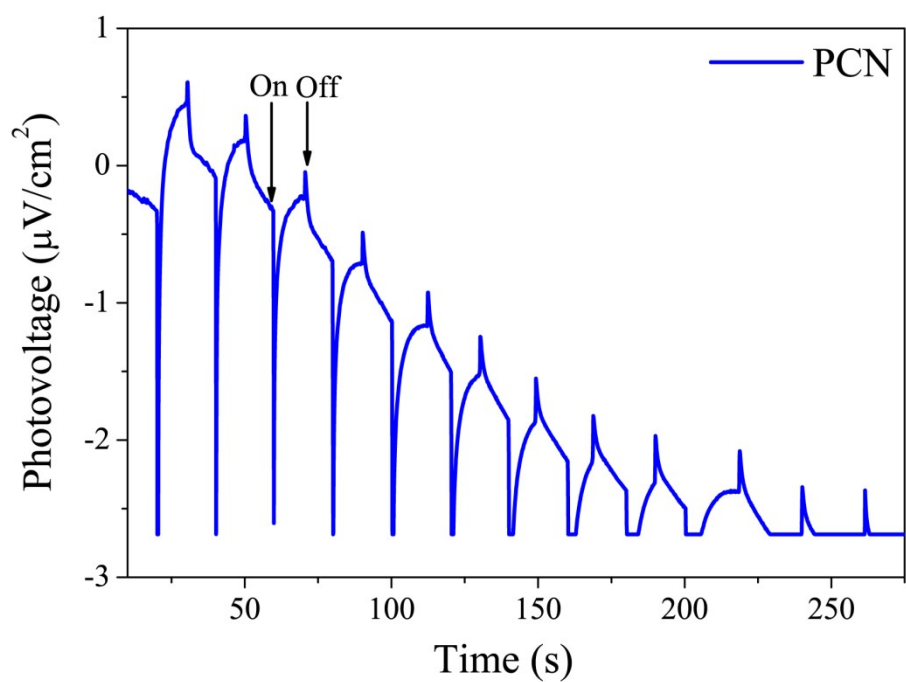
Figure S10 Photocurrent responses of OCN and PCN/OCN.
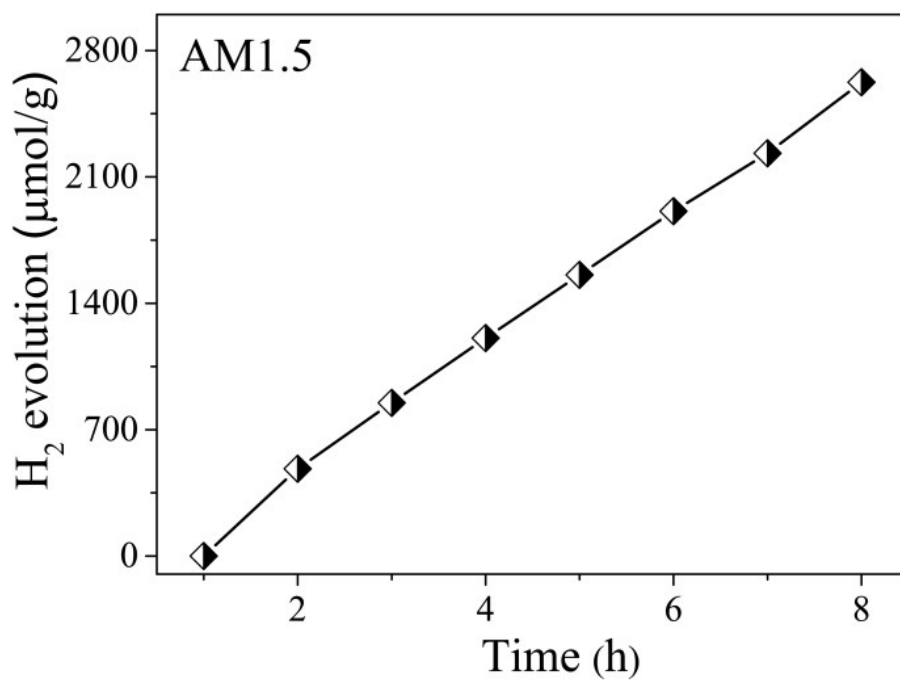

Figure S11. Photocurrent response of PCN.

Figure S12. H_2 generation activities of PCN/OCN under xenon lamp irradiation (AM1.5G), with photo-deposition of 1% Pt as cocatalyst.
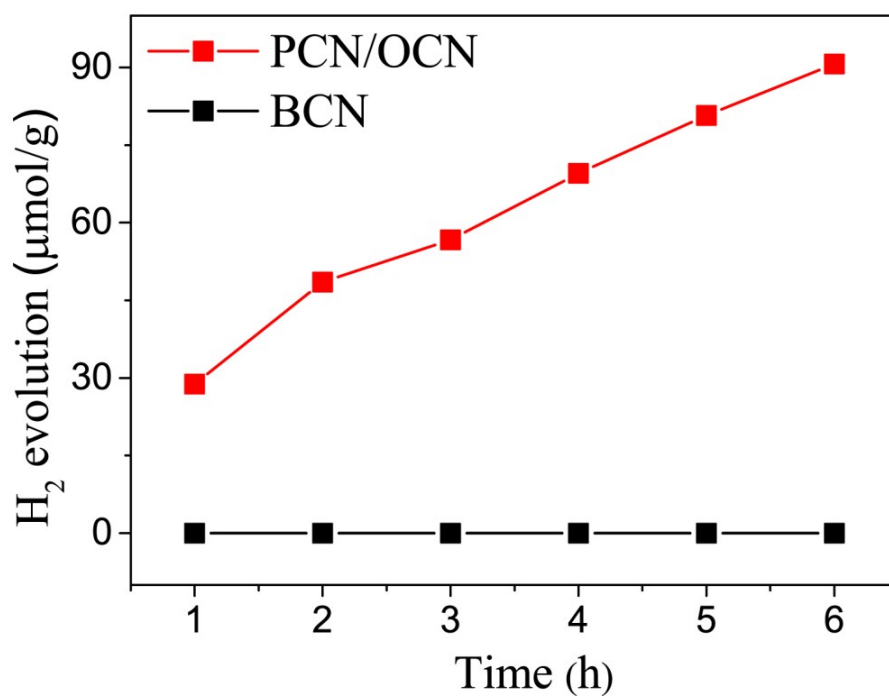

Figure S13. H_2 generation activities of PCN/OCN and BCN under Xenon lamp irradiation (320-780 nm) without Pt cocatalyst.
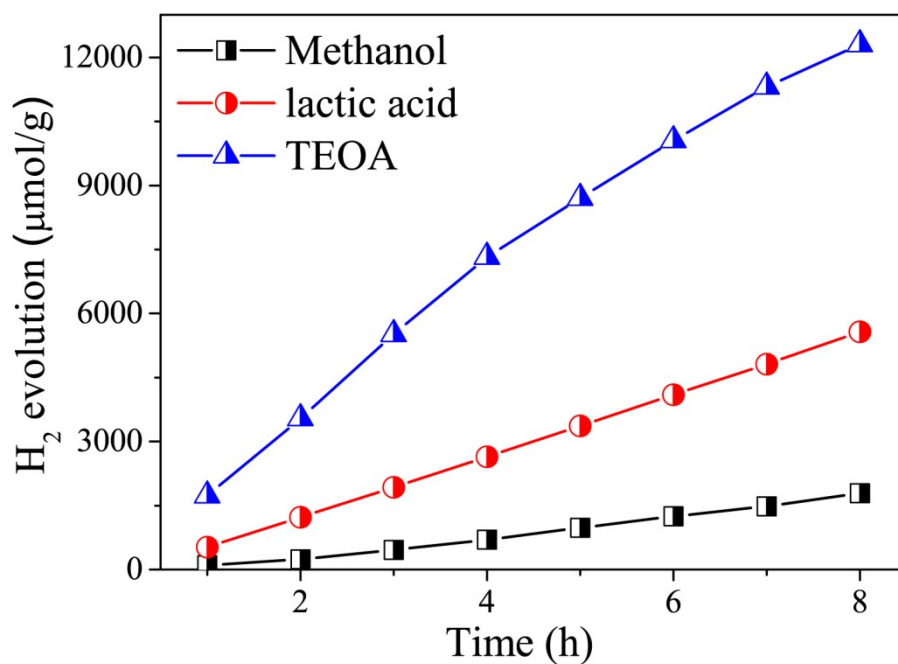
Figure 14. A comparison of photocatalytic hydrogen production of PCN/OCN at different sacrificial reagents.
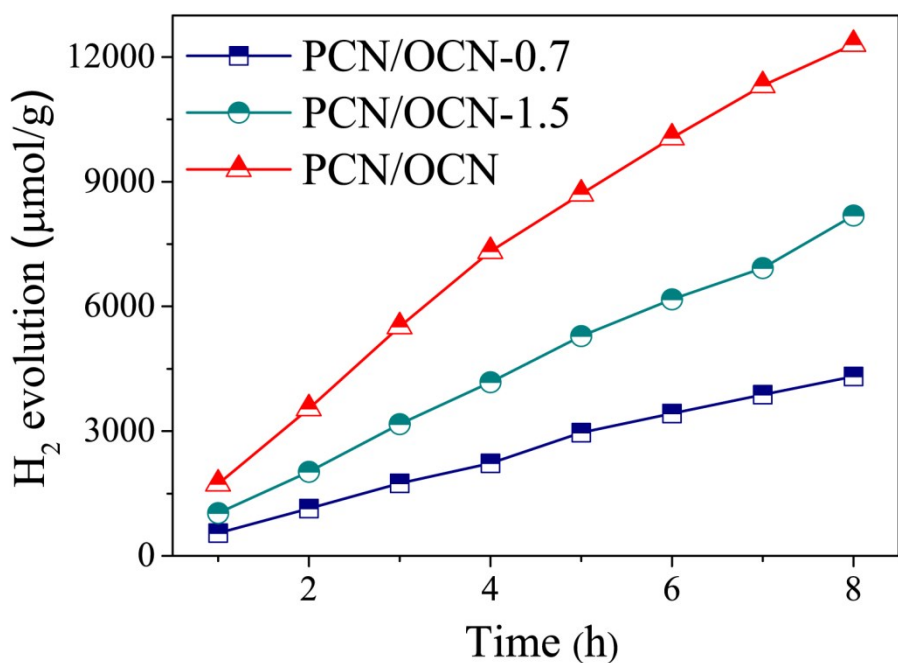

Figure S15. H_2 generation activities of different mass ratio of PCN/OCN under xenon lamp irradiation (320-780 nm), with photo-deposition of 1% Pt as cocatalyst.
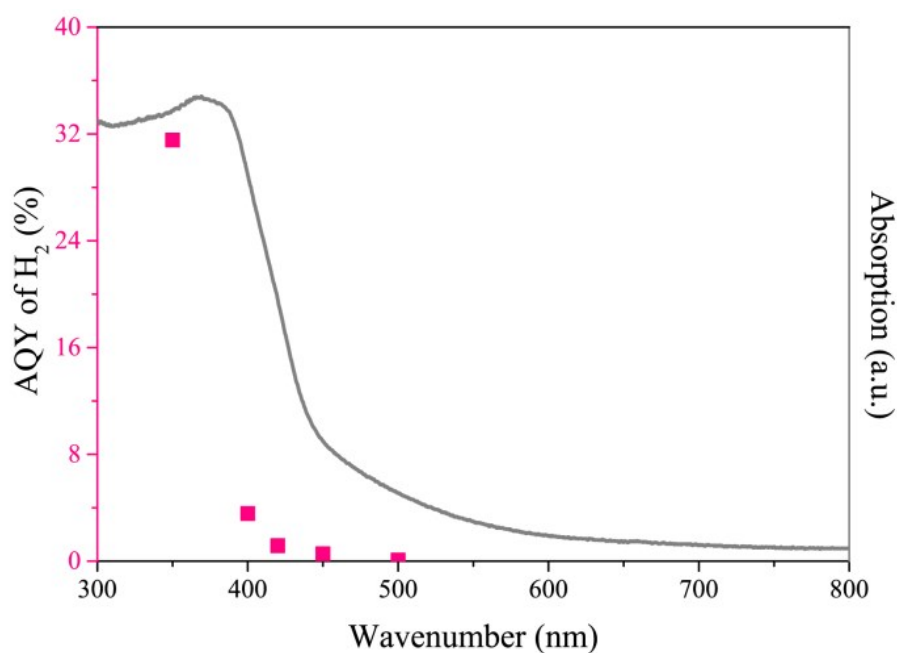
Figure S16. UV-vis spectrum (black line) and AQY of H_2 (pink dots) at different wavelengths on PCN/OCN in the presence of 10% TEOA as a hole scavenger and 1% Pt as the cacatalyst.

Table S1. AQY data of PCN/OCN and BCN samples at different wavelengths

Wavenumber (nm)	350	400	420	450	500
AQY(PCN/OCN)/%	31.56	3.57	1.16	0.57	0.10
AQY(BCN)/%	6.13	0.42	0.17	0.03	0

Table S2. H_2 production data of the samples loaded with 1% Pt

Samples	Activity/ mmol g^{-1}h^{-1} [a]	Activity/ mmol g^{-1}$_{[Pt]}$h^{-1} [b]	TON$_{[Pt]}$ (8 h) [c]
PCN/OCN	1.54	153.8	240
BCN	0.19	19.3	30
PCN	0.44	43.8	68
OCN	0.52	51.8	81
PCN/OCN-0.7	0.54	54.0	84
PCN/OCN-1.5	1.02	102.3	160
BOCN	0.27	26.7	42
Physically mixed	0.56	56.5	88

[a]=(H_2 amount in 8h/total mass of catalysts)/8h

[b]=H_2 amount vs. Pt loading mass= [a]/Pt loading mass fraction=[a]/0.01

[c] H_2 amount vs. Pt loading amount=[b]*8*195.08/1000

The calculated AQY of PCN/OCN was about 31.56, 3.57, 1.16, 0.57 and 0.10 % at 350, 400, 420, 450 and 500 nm (Figure S16 and Table S1), respectively. AQY value of PCN/OCN at 400 nm is about 8.5 times higher than that of BCN. $TON_{[Pt]}$ of all samples were calculated and listed in Table S2. By comparison, PCN/OCN shows the highest $TON_{[Pt]}$ of 240 after 8 h.
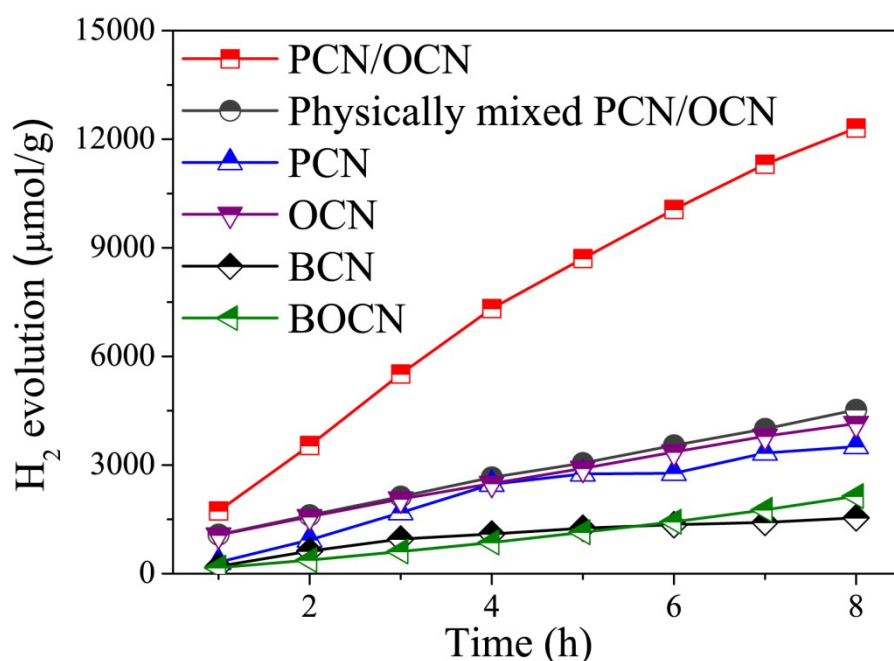

Figure S17. H_2 generation activities of given samples under Xenon lamp irradiation (320-780 nm), with photo-deposition of 1% Pt as cocatalyst.
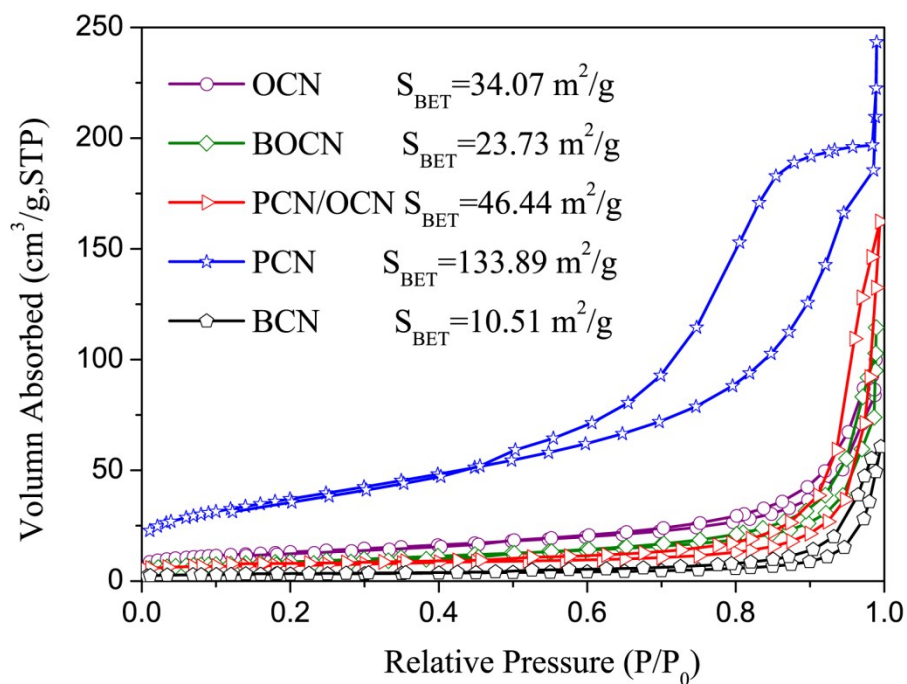
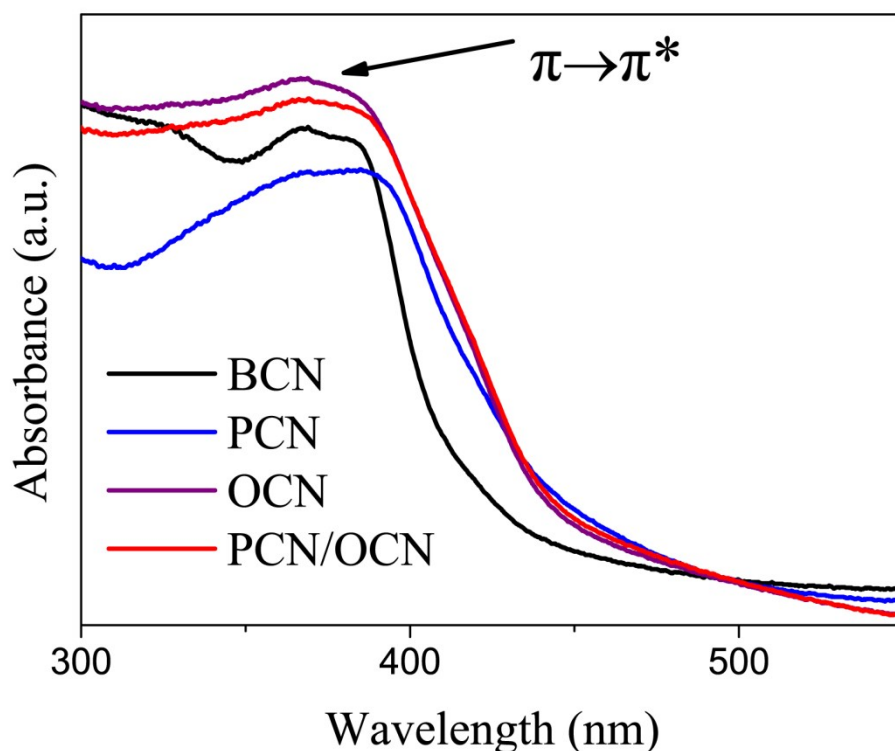Figure S18. Nitrogen adsorption-desorption isotherms of PCN, OCN, BCN, BOCN, PCN/OCN samples.

Figure S19. UV-Vis DRS spectra of BCN, PCN, OCN, PCN/OCN samples. The absorption edges of BCN, PCN, OCN and PCN/OCN are 420, 450, 451, 455 nm, respectively. In contrast to BCN, the others samples showed remarkably red shift in

absorption edge. The red shift of absorption edge of PCN was resulted from the enhancement of conjugate effect due to the increased crystallinity, but OCN is attributed to the introduction of impurity energy level because of O elemental doping.
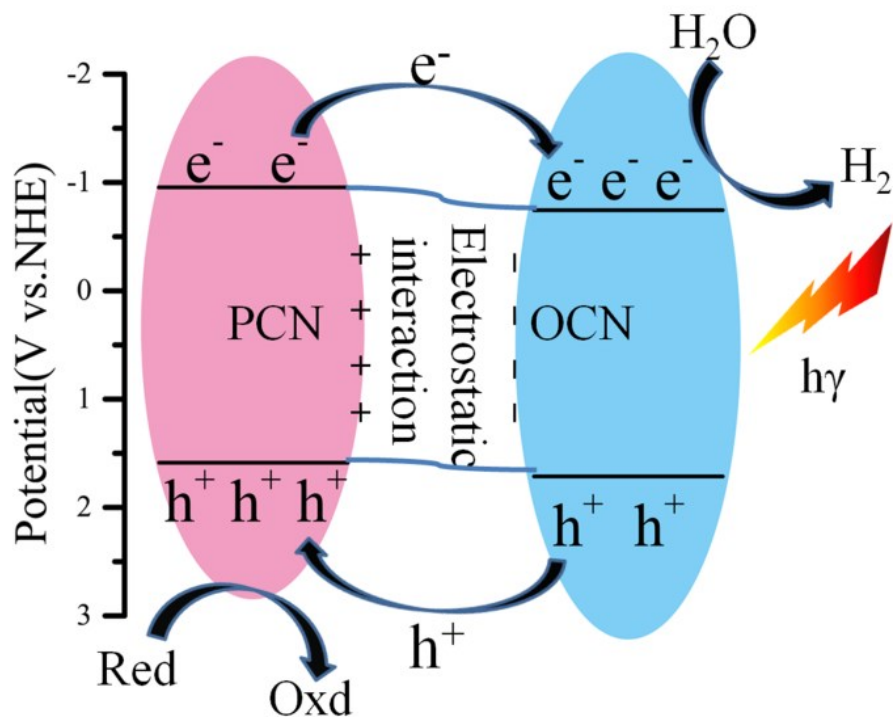

Figure S20. Proposed mechanism of photocatalytic hydrogen evolution in the presence of PCN/OCN.

Table S3 A comparison of photocatalytic water splitting activity of g-C_3N_4 based phocatalysts

Photocatalytic system	Light source	Reaction solution	Co-catalyst (wt% Pt)	Fabrication strategy	H_2 generation rate ($umol \cdot g^{-1} \cdot h^{-1}$)	Refs
PCN/OCN	300 W Xe lamp (320-780nm)	50 mL aqueous solution containing TEOA (10 vol%)	1	electrostatic self-assembly	1538.3	This work
PCN/OCN	300 W Xe lamp (>420nm)	50 mL aqueous solution containing TEOA (10 vol%)	1	electrostatic self-assembly	663	This work
Meso-g-C_3N_4/g-C_3N_4	300 W Xe lamp (AM 1.5G filter)	100 mL aqueous solution containing methanol (20%)	No data	template-calcination strategy	115.6	S1
triazine-/heptazine based g-C_3N_4	300 W Xe lamp (>420nm)	100 mL aqueous solution containing TEOA (10 vol%)	3	one-step molten salt	661	S2
1D-2D g-C_3N_4	150 W metal halide lamp	100 mL aqueous solution containing TEOA (10 vol%)	0.5	two-step condensation method	241	S3
MCN/UCN	300 W Xe lamp (>420nm)	100 mL aqueous solution containing TEOA (15 vol%)	1	hydrothermal +calcination	598	S4
Ti_3C_2/g-C_3N_4	200 W Hg lamp (>400nm)	40 mL aqueous solution containing TEOA (10 vol%)	3	electrostatic self-assembly approach	72.3	S5

References

[S1]   S. Y. Tan, Z. P. Xing, J. Q. Zhang, Z. Z. Li , X. Y. Wu, J. Y. Cui, J. Y. Kuang, J. W. Yin and W. Zhou, Int. J. Hydrog. Energy, 2017, **42**, 25969-25979.

[S2]   J. Yang, Y. J. Liang, K. Li, G. Yang, K. Wang, R. Xu and X. J. Xie, Appl. Catal. B, 2020, **262**, 118252

[S3]   S. Mahzoon, S. M. Nowee, M. Haghighi. Renew. Energ. 2018, **127**, 433-443

[S4]   Q. L. Xu, D. K. Ma, S. B. Yang, Z. F. Tian, B. Cheng and J. J. Fan. Appl. Surf. Sci., 2019, **495**, 143555

[S5]   T. M. Su, Z. D. Hood, M. Naguib, L. Bai, S. Luo, C. M. Rouleau, I. N. Ivanov, H. B. Ji, Z. Z. Qin and Z. L. Wu, Nanoscale, 2019, **11**, 8138